

Research Article

Dry Deposition of PM_{2.5} Nitrate in a Forest according to Vertical Profile Measurements

Mao Xu, Kazuhide Matsuda*

United Graduate School of Agricultural Science, Tokyo University of Agriculture and Technology, 3-5-8 Saiwai-cho, Fuchu, Tokyo 183-8509, Japan

***Corresponding author.**

Tel: +81-42-367-5818

E-mail: kmatsuda@cc.tuat.ac.jp

Received: 26 May 2020

Revised: 17 August 2020

Accepted: 19 August 2020

ABSTRACT The atmospheric nitrogen compounds can serve as a nutrient; however, its excess deposition has harmful effects on terrestrial ecosystems due to acidification and eutrophication. There are still large uncertainties concerning the dry deposition process of PM_{2.5} nitrate in forests, even though this process affects the accuracy of chemical transport model simulations. To better understand this process, we conducted vertical profile measurements of inorganic ions in PM_{2.5} and SO₂ above and within a forest canopy in the Field Museum Tamakyuryo site in suburban Tokyo with a particular focus on the processes observed under both daytime and nighttime and both leafy and leafless conditions. We performed two observations during leafy periods (July 21–August 1, 2015, and September 27–October 11, 2016) and one observation during a leafless period (February 23–29, 2016). To obtain daytime and nighttime vertical profiles, we set filter holders at 4 or 5 heights on an observation tower in the forest and changed the filters for each daytime and nighttime. For the PM_{2.5}, the vertical gradients of NO₃⁻ concentration were larger than those of SO₄²⁻ during both the daytime and nighttime for all observational periods, particularly during the leafy periods. In addition, the decreasing rate of NO₃⁻ in the PM_{2.5} within the canopy was larger than that of SO₂ for some observational periods. In the daytime, the air temperature was higher near the canopy surface during the leafy period and near the ground surface during the leafless period. As also suggested by past studies, the large gradients of NO₃⁻ in the PM_{2.5} during the leafy period were likely caused by the volatilization of NH₄NO₃ near the deposition surfaces due to the higher temperature in the daytime and the lower concentration of HNO₃ caused by its fast removal during both the daytime and nighttime.

KEY WORDS Air-surface exchange, Gradient, Semi-volatile aerosols, Ammonium nitrate, Leaf area

1. INTRODUCTION

A drastic increase in the emission of nitrogen compounds on a global scale has occurred due to human activities over the last century (Galloway *et al.*, 2008). In particular, a drastic increase in the emission of nitrogen oxides (NO_x) associated with energy consumption has been observed over East Asia in recent decades (Kurokawa *et al.*, 2013; Ohara *et al.*, 2007). NO_x acts as a precursor of nitrate atmospheric particulate matter with diameters of less than 2.5 μm (PM_{2.5}); such particu-

late matter is known to have adverse effects on human health. Moreover, these nitrogen compounds have harmful effects on terrestrial ecosystems due to acidification and eutrophication via the deposition of excess nitrogen.

PM_{2.5} simulations have been conducted using chemical transport models over Japan (Shimadera *et al.*, 2018; Morino *et al.*, 2015; Shimadera *et al.*, 2014); however, such models have clearly overestimated the concentration of NO₃⁻ in PM_{2.5}. Shimadera *et al.* (2014) suggested that the simulated concentration was highly dependent on the uncertainty in the dry deposition process of nitrogen compounds. Moreover, for NO₃⁻ in PM_{2.5}, large uncertainties exist in the theoretical models used to estimate the dry deposition rates, particularly on forest surfaces (Flechard *et al.*, 2011). However, the dry deposition process of PM_{2.5} has rarely been studied in East Asia, where anthropogenic emissions of NO_x are higher than those found in Europe and North America. Therefore, a better understanding of the dry deposition process of NO₃⁻ in PM_{2.5} in this region will contribute to improving the model accuracy of estimated PM_{2.5} concentrations and nitrogen deposition rates.

Several field experiments to determine the deposition velocity (V_d) of PM_{2.5} nitrate in forests via gradient or relaxed eddy accumulation methods have been performed in Japan (Sakamoto *et al.*, 2018; Honjo *et al.*, 2016; Takahashi and Wakamatsu, 2004). These experiments suggest that the equilibrium shift of NH₄NO₃ into the gas phase likely enhances the dry deposition of nitrogen compounds, as indicated by previous studies in other regions (Nemitz *et al.*, 2004; Wyers and Duyzer, 1997; Sievering *et al.*, 1994; Huebert *et al.*, 1988). Measurements of the vertical profiles of relevant matter are useful to understand dry deposition mechanisms in forests. Yamazaki *et al.* (2015) found different vertical profiles for NO₃⁻ and SO₄²⁻ in PM_{2.5} in a forest in Tokyo over the course of a year, likely due to the abovementioned volatilization process. However, these studies conducted in Japan primarily focused on leafy forests and did not examine the diurnal deposition process. To improve the understanding of dry deposition processes for PM_{2.5} in East Asia further, we conducted intensive field observations in a forest in suburban Tokyo. We obtained the vertical profiles of the PM_{2.5} components together with those of SO₂, a stereotypical gas, the deposition processes of which have been generalized (Nemitz, 2015), to compare the differences in the deposition processes of particle and gaseous matter. We particularly focused on

the daytime and nighttime deposition processes of PM_{2.5} in a forest during leafy and leafless periods.

2. OBSERVATIONS AND METHODOLOGY

We conducted the measurements using an observation tower (Fig. 1) in a forest at the Field Museum Tamakyuryo (FM Tama) site of the Tokyo University of Agriculture and Technology, which is located in a western suburb of Tokyo, Japan (35°38'N, 139°23'E). Deciduous trees (*Quercus*) were the dominant tree species around the tower in addition to some Japanese cedar (*Cryptomeria*). The canopy height around the tower was approximately 20 m. The deciduous trees were leafy from April and leafless from December. Other details concerning the measurement site have been described in Matsuda *et al.* (2015).

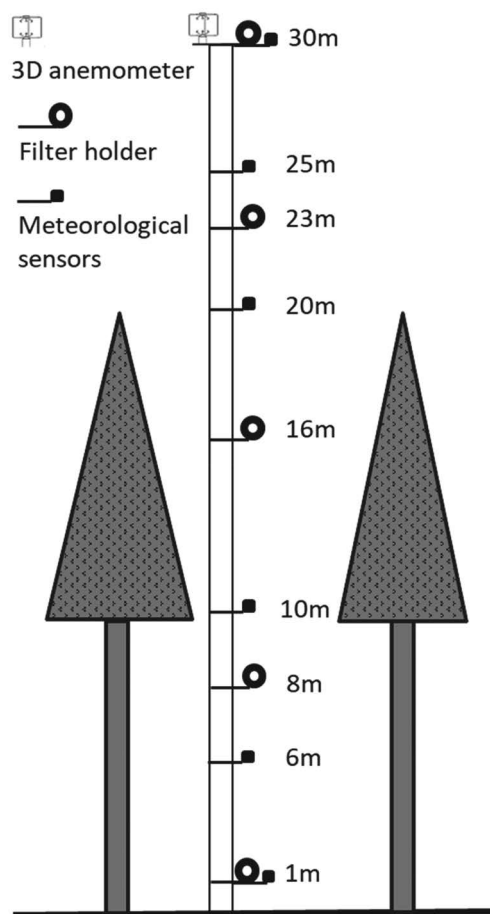


Fig. 1. Schematic diagram of the observation tower at the Field Museum Tamakyuryo site.

Table 1. Experimental periods and sampling strategies.

Season	Experimental period	Daytime sampling	Nighttime sampling	Measurement heights
Summer (leafy)	July 21–August 1, 2015	06:00–18:00	18:00–06:00	30 m, 23 m, 8 m, 1 m
Winter (leafless)	February 23–29, 2016	08:00–17:00	17:00–08:00	
Autumn (leafy)	September 27–October 11, 2016			30 m, 23 m, 16 m, 8 m, 1 m

Table 2. Atmospheric conditions at a height of 30 m at the tower and the leaf area index. WS, Temp, RH, and LAI indicate the wind speed, temperature, relative humidity, and leaf area index, respectively. All values except LAI are given as the average \pm standard deviation from the 10-min means of the data for the meteorological parameters and the half-day data for the concentrations.

Experiment	WS (m s ⁻¹)	Temp (°C)	RH (%)	Concentration ($\mu\text{g m}^{-3}$)		LAI
				SO ₄ ²⁻	NO ₃ ⁻	
Summer 2015 (15-summer)						4.4
Daytime	3.1 \pm 2.4	29.2 \pm 2.3	64 \pm 11	6.3 \pm 4.0	0.6 \pm 0.4	
Nighttime	2.8 \pm 1.5	26.6 \pm 1.7	77 \pm 9	6.7 \pm 4.8	1.9 \pm 1.3	
Winter 2016 (16-winter)						1.7
Daytime	3.4 \pm 2.1	6.5 \pm 3.4	45 \pm 18	2.6 \pm 1.5	2.9 \pm 1.3	
Nighttime	2.8 \pm 1.4	4.0 \pm 2.9	65 \pm 15	3.0 \pm 2.1	3.7 \pm 1.2	
Autumn 2016 (16-autumn)						4.3
Daytime	1.8 \pm 0.7	25.7 \pm 3.2	61 \pm 14	2.0 \pm 1.3	1.5 \pm 0.8	
Nighttime	2.9 \pm 2.1	20.9 \pm 3.8	71 \pm 16	2.1 \pm 1.2	1.0 \pm 0.7	

We performed two observations during leafy periods and one during a leafless period from July 2015 to October 2016. We sampled PM_{2.5} and SO₂ simultaneously using a filter pack (Tokyo Dylec Corporation, NILU filter folder NL-O) with an impactor and a pump unit (Tokyo Dylec Corporation, MCI sampler). The flow rate was set to 20 L min⁻¹ in accordance with the PM_{2.5} cut off the impactor. PM_{2.5} was collected on glass fiber filters coated with Teflon. SO₂ was collected on a cellulose filter impregnated with potassium carbonate following the PM_{2.5} filter. To obtain vertical concentration profiles during the daytime and nighttime, we set the filter holders at four or five heights, as indicated in Table 1, on the tower and changed the filters twice a day. Outlines of the samplings during each observational period are given in Table 1. To sufficiently detect the vertical gradients, we set the sampling time to more than 9 h after considering previous measurements at the same site (Yamazaki *et al.*, 2015). Sampling was conducted continuously, except when it was raining. We obtained 36 valid samples in total at each height level. After the samples were collected, the inorganic ions in each filter were extracted into

deionized water via ultrasonic extraction and then analyzed using ion chromatography (Thermo Scientific, Dionex ICS-1100).

Meteorological conditions including the wind speed (WS), temperature (Temp), and relative humidity (RH) were observed at heights of 30 m, 25 m, 20 m, 10 m, 6 m, and 1 m along the tower using meteorological sensors (YOUNG 81000 and PREDE PHMP45A at 30 m; VAISALA WXT520 at 25 m, 20 m, 10 m, 6 m, and 1 m). The 10-min averages were used to obtain the vertical profiles of each parameter. The leaf area index (LAI) was measured using a plant canopy analyzer (LI-COR LAI-2200).

3. RESULTS AND DISCUSSION

3.1. Overview of the Three Observational Periods

Table 2 shows the atmospheric conditions at the observation site for the three periods considered here. The estimated LAI shows a leafy canopy in 15-summer and 16-autumn and a leafless canopy in 16-winter, where

15-summer, 16-autumn, and 16-winter indicate the three observational periods during the summer of 2015, the autumn of 2016, and the winter of 2016, respectively. The WS values were highest during the daytime in 16-winter; the Temp values were highest during the daytime in 15-summer; and the RH values were highest during the nighttime in 15-summer. The concentrations of SO_4^{2-} in the $\text{PM}_{2.5}$ were highest in 15-summer, while the concentrations of NO_3^- in the $\text{PM}_{2.5}$ were highest in 16-winter. In the three experiments, 78–83% of the inorganic ions in the $\text{PM}_{2.5}$ consisted of NH_4^+ , SO_4^{2-} , and NO_3^- . The results were broadly similar at all heights. According to the relationship between the equivalent concentrations of NH_4^+ and $\text{SO}_4^{2-} + \text{NO}_3^-$ in each $\text{PM}_{2.5}$ profile, the inorganic components primarily existed as $(\text{NH}_4)_2\text{SO}_4$ or NH_4NO_3 .

The temporal variations in the mass concentrations of SO_4^{2-} and NO_3^- in the $\text{PM}_{2.5}$ at heights of 30 m, 23 m, 8 m, and 1 m during the observational periods are shown in Fig. 2. During the three observational periods, there were no significant differences in the mass concentrations of SO_4^{2-} between these heights except between 8 m and 1 m ($p < 0.01$), but there were significant differences in the mass concentrations of NO_3^- ($p < 0.01$). The NO_3^- concentration clearly decreased from the top of the canopy to the forest floor during the observations compared to the SO_4^{2-} concentration.

3.2 Vertical Profiles and Decreasing Rates

The vertical concentration profiles of SO_4^{2-} and NO_3^- in the $\text{PM}_{2.5}$ and those of SO_2 during the daytime and nighttime for the observational periods are shown in Fig. 3. The daytime and nighttime averages at each height were used to obtain the vertical profiles. The concentrations at all heights were normalized by those at 30 m. In general, the dry deposition mechanisms of aerosols are thought to depend on the physical processes at each particle size. In that case, the vertical profiles of SO_4^{2-} and NO_3^- in the $\text{PM}_{2.5}$ should show similar tendencies. However, the decreasing trend of NO_3^- below the canopy was clearly larger than that of SO_4^{2-} during both the daytime and nighttime for all observational periods, especially during the leafy seasons (15-summer and 16-autumn). In the leafless season (16-winter), the differences in the SO_4^{2-} and NO_3^- vertical profiles decreased due to the smaller decrease in NO_3^- .

The decreasing rate (hereafter referred to as *DR*) is a proper index to understand the tendency of whether the

target component is removed or not between each of the heights. The *DR* is defined as the following:

$$DR = (C_{z_1} - C_{z_0}) / C_{z_1} \quad (1)$$

where C_{z_1} and C_{z_0} is the concentration of the target component at z_1 [m] and z_0 [m] ($z_1 > z_0$), respectively. Therefore, differences in *DR* indicate the differences in the removal efficiency between components. Because SO_2 is a gas that is easy to deposit on forest surfaces due to its reactive and water-soluble properties, its value of *DR* is assumed larger than that of fine particulate matter (e.g., Erisman and Draaijers, 1995). This assumption holds between SO_2 and SO_4^{2-} for all observations in the canopy. However, the *DR* value of NO_3^- below the canopy was larger than that of SO_2 during some observational periods (daytime in 15-summer and 16-autumn) (Fig. 3). Therefore, there are likely other factors that enhance the deposition of NO_3^- in $\text{PM}_{2.5}$ in addition to physical processes.

The DR_{30-1} values (the *DR* values between 30 m and 1 m) of SO_4^{2-} and NO_3^- for the observational periods are shown in Fig. 4. Each circle shows a daytime or nighttime daily value. The DR_{30-1} values of NO_3^- were clearly larger than those of SO_4^{2-} , particularly in 15-summer and 16-autumn. The DR_{30-1} values of SO_4^{2-} varied independently of LAI for all observations. Conversely, the DR_{30-1} values of NO_3^- were clearly larger during the leafy periods and smaller during the leafless period. These results indicate that the variation in the NO_3^- decrease may be closely related to the leaf condition. In effect, the removal efficiency of NO_3^- by the leaf canopy was larger than that of SO_4^{2-} regardless of the time of day.

3.3 Effect of the Equilibrium Shift of NH_4NO_3 on the Deposition Process

$(\text{NH}_4)_2\text{SO}_4$ particles have a very low vapor pressure and exist as an aerosol under atmospheric conditions. Conversely, NH_4NO_3 particles are semi-volatile and have an equilibrium relationship with NH_3 and HNO_3 in the atmosphere. The dry deposition of NH_4NO_3 is affected by its volatilization process and depends on Temp, RH, and the concentrations of either HNO_3 or NH_3 . Therefore, differences in the DR_{30-1} values between SO_4^{2-} and NO_3^- were likely caused by differences in their chemical properties.

There are some previous studies mentioned below that indicate a higher V_d value for NO_3^- particles compared to SO_4^{2-} particles. For a crested wheatgrass field in the Boul-

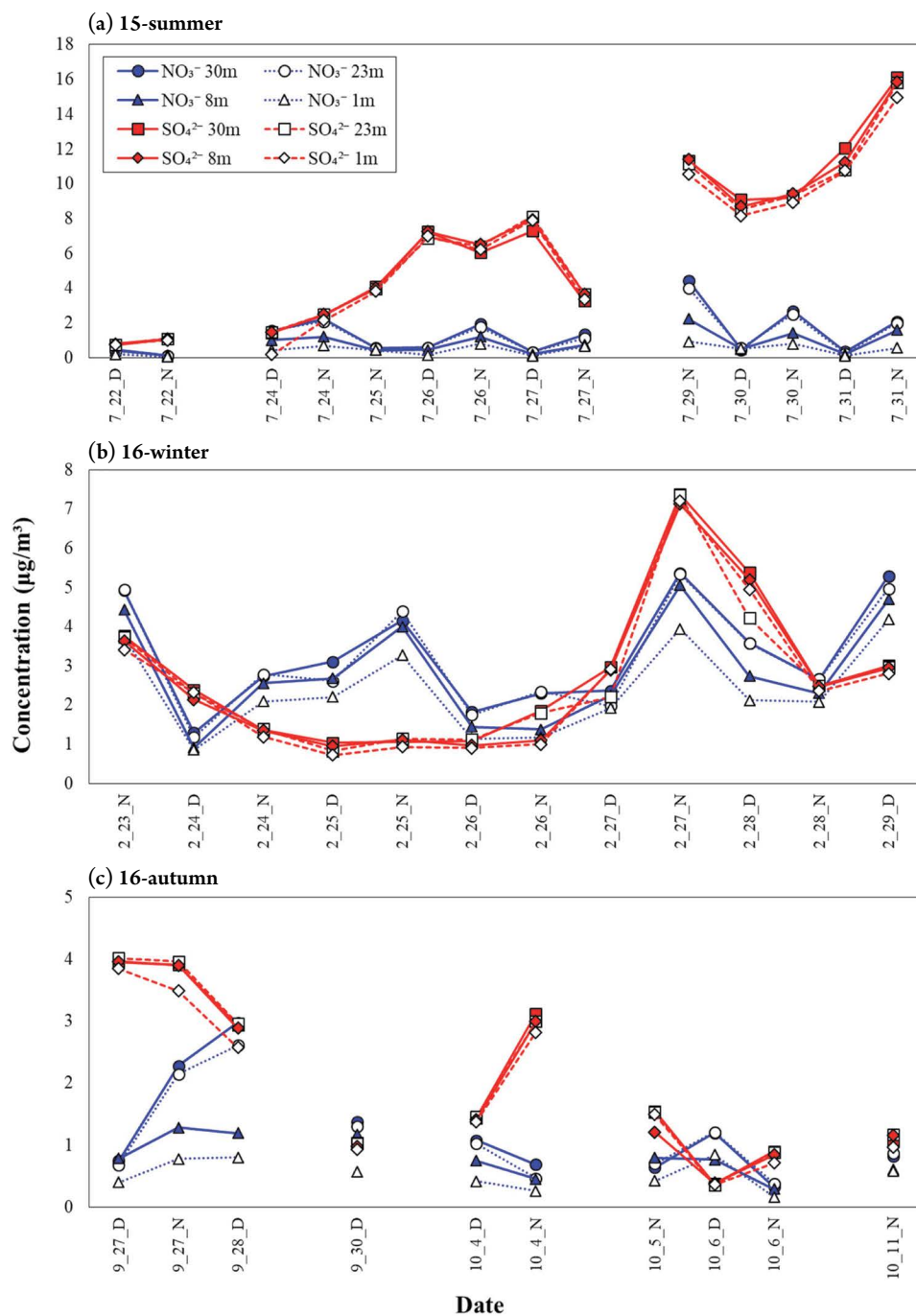


Fig. 2. Temporal variations in the mass concentrations of SO_4^{2-} and NO_3^- in the $\text{PM}_{2.5}$ at 30 m, 23 m, 8 m, and 1 m at the tower during the three observational periods. D and N indicate daytime and nighttime, respectively.

der Atmospheric Observatory, a research facility in Colorado in the United States, Huebert *et al.* (1988) found that the vertical gradients of the NO_3^- concentrations in particles were larger than those of SO_4^{2-} and sometimes exceeded those of HNO_3 , which has a very high V_d value.

These results are consistent with the predictions of a model coupling the volatilization of NH_4NO_3 to the rapid dry deposition of HNO_3 presented in Brost *et al.* (1988). Wyers and Duyzer (1993) determined the V_d values of SO_4^{2-} and NO_3^- above a coniferous forest in

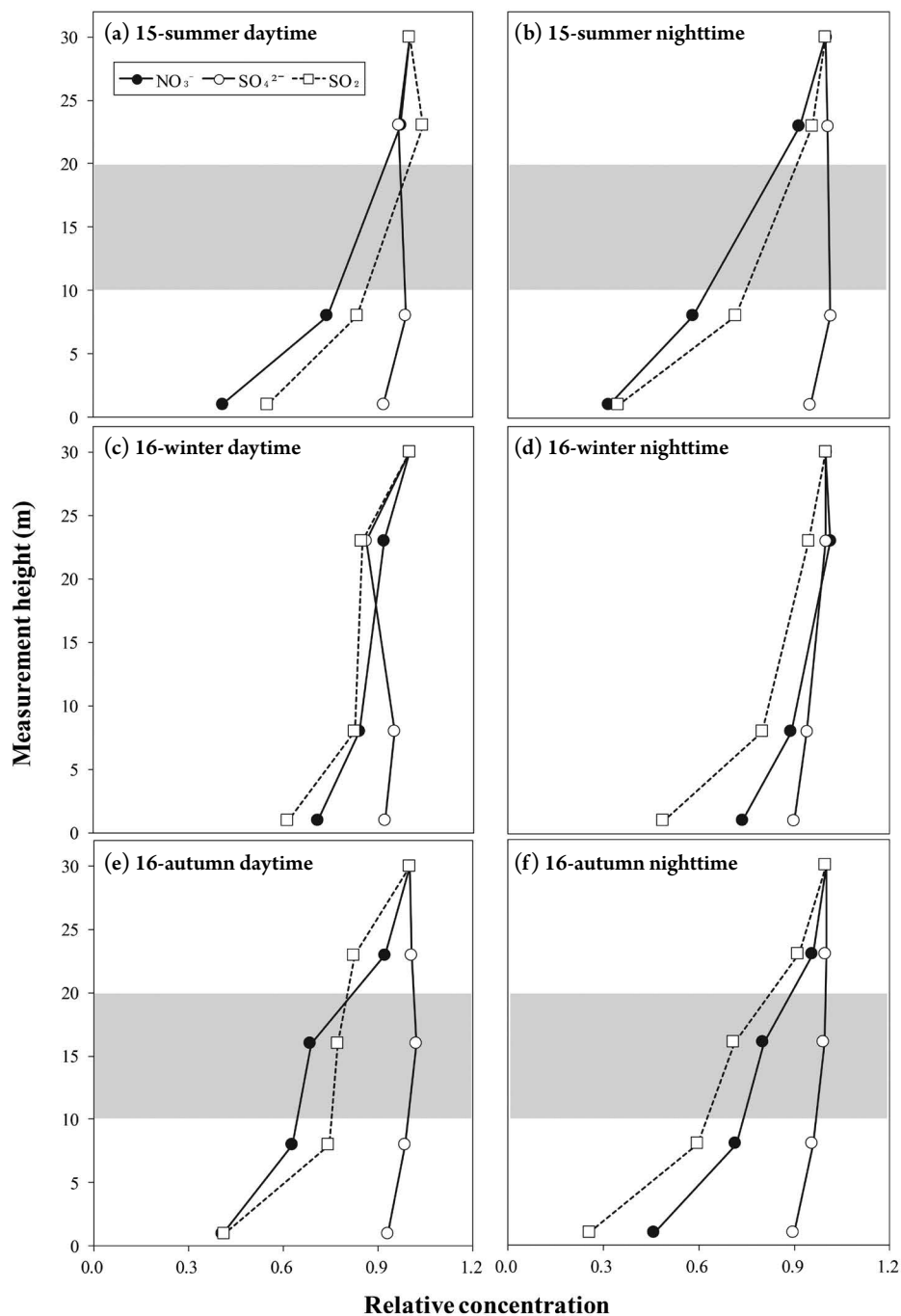


Fig. 3. Normalized vertical profiles of the mass concentrations of SO_4^{2-} in the $\text{PM}_{2.5}$ (open circles), NO_3^- in the $\text{PM}_{2.5}$ (closed circles), and SO_2 (open squares) during the daytime and nighttime for the three observational periods. The relative concentration is the concentration ratio with respect to the concentration at 30 m. The gray layers indicate the leafy canopies.

Speulderbos in the Netherlands using the gradient method. They found that the V_d value of NO_3^- was larger than that of the maximum theoretically possible value when the temperature was high (above 20°C) and much larger

than that of SO_4^{2-} , possibly due to the equilibrium shift from NH_4NO_3 to NH_3 and HNO_3 . Van Oss *et al.* (1998) used these results in their simulations, which considered the influence of the gas-to-particle conversion on surface

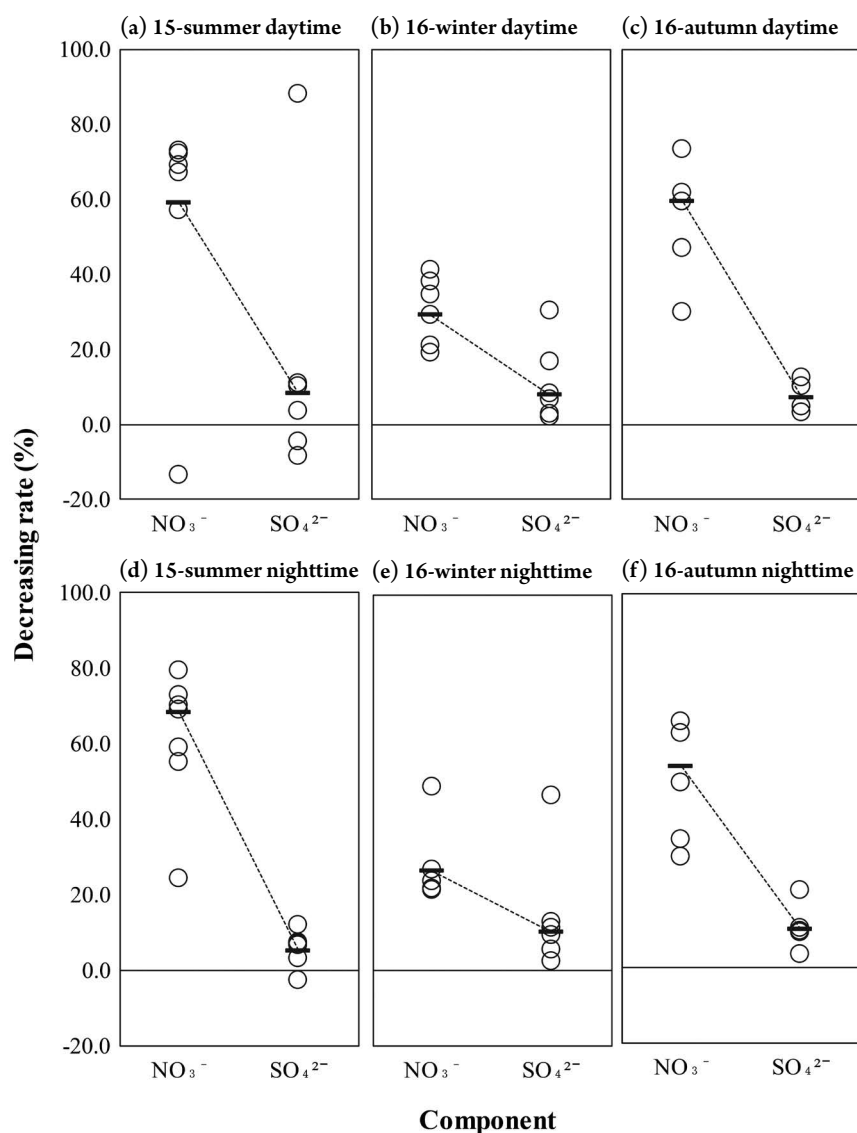


Fig. 4. Distributions of the decreasing rates of SO_4^{2-} and NO_3^- in the $\text{PM}_{2.5}$ from 30 m to 1 m for the three observational periods. Each circle shows a daytime or nighttime daily value. The bars indicate the mean values.

exchange processes above a forest. Their simulation results suggest that the volatilization of particulate NH_4NO_3 during the daytime can lead to the emission of HNO_3 and NH_3 above the forest, along with the observed anomalously large V_d value for NO_3^- compared to the theoretical value. Based on the observations in Nemiz *et al.* (2004) of a dry inland heath dominated by *Calluna vulgaris* in Elspeetsche Veld in the Netherlands, the surface concentration products of HNO_3 and NH_3 were well below the thermodynamic equilibrium value and the Damköhler numbers indicated that the chemical conversion was sufficiently fast to modify the exchange fluxes.

Considering these studies, there are two possible sources of the differences in the dry deposition mechanisms between $(\text{NH}_4)_2\text{SO}_4$ and NH_4NO_3 :

- (1) An equilibrium shift of NH_4NO_3 due to the higher temperature near the deposition surfaces and/or
- (2) An equilibrium shift of NH_4NO_3 due to the low concentrations of HNO_3 caused by fast removal near the deposition surfaces.

The variations in the ensemble mean air temperature over the observational periods are shown in Fig. 5. In the daytime, Temp at 30 m was lower than Temp at 20 m, which was close to the canopy surface during 15-sum-

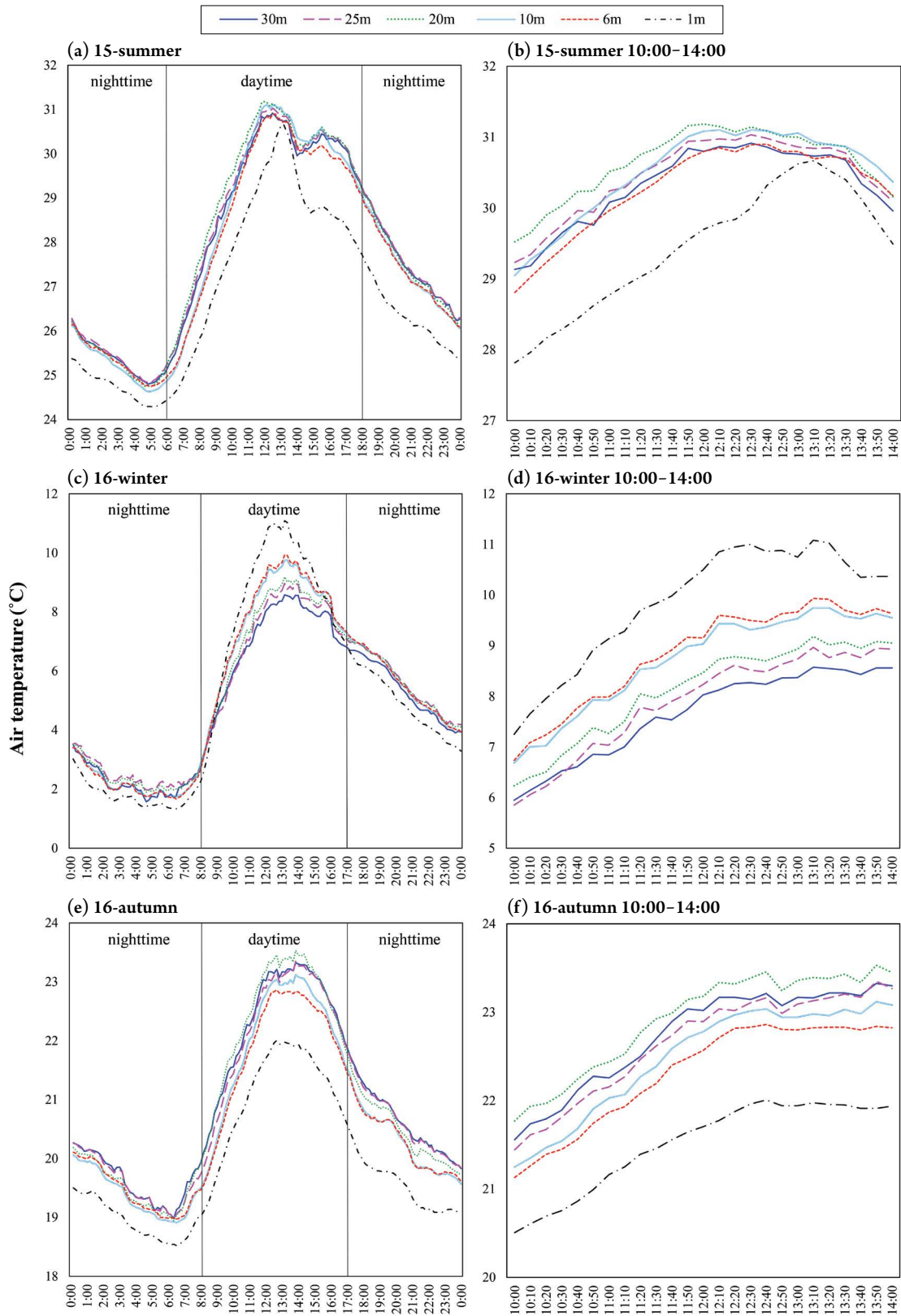


Fig. 5. Variations in the ensemble mean values of the air temperature at 30 m, 25 m, 20 m, 10 m, 6 m, and 1 m for the three observational periods. The figures ((b), (d), (f)) are an expansion of the period from 10:00 to 14:00.

mer and 16-autumn, and was lower than Temp at 1 m, which was close to the ground surface during 16-winter. This occurred because direct sunlight struck the canopy surface during the daytime in the leafy periods (15-summer and 16-autumn) while it struck the ground surface in the leafless period (16-winter). In addition, Temp values of forest surfaces exposed to sunlight tend to be higher than the Temp values near the surfaces (Nakahara *et al.*, 2019). Therefore, the volatilization of NH₄NO₃ was likely enhanced close to the canopy surface during the leafy periods and close to the ground surface during the leafless period. This is in agreement with the higher daytime DR₃₀₋₁ values of NO₃⁻ than SO₄²⁻ during the three periods (Fig. 4). Conversely, the air temperature gradients mentioned above were not clearly seen in the nighttime data during the three periods, even though the DR₃₀₋₁ values of NO₃⁻ were also higher than SO₄²⁻ in the nighttime. The NH₄NO₃ aerosols have an equilibrium relationship with the concentrations of the HNO₃ and NH₃ gases in the atmosphere. The V_d value of HNO₃ is known to be greatly higher than those of NH₃ and NH₄NO₃. The V_d values calculated by the resistance models are 3–10 times higher than those of other gaseous and particulate matter (Ban *et al.*, 2016). During the leafy periods, HNO₃ was quickly removed by the canopy surface due to the high V_d values and the large leaf area. When HNO₃ is quickly removed by deposition surfaces, its concentration near these surfaces drastically decreases. Then, the gas-particle equilibrium is shifted to the gas phase. After that, NH₄NO₃ near the surfaces volatilizes to resupply the decreased level of HNO₃ and quickly deposits to the surfaces as gaseous matter. This can cause a high DR₃₀₋₁ value for NO₃⁻ not only in the daytime but also in the nighttime. This is likely because NH₄NO₃ can be removed from the atmosphere just as quickly as SO₂ (Fig. 3) and therefore the DR₃₀₋₁ value of NH₄NO₃ can become significantly larger than that of (NH₄)₂SO₄ (p < 0.01) (Fig. 4).

Katata *et al.* (2020) applied a new multi-layer land surface model, which was coupled with the NH₄NO₃ gas-particle conversion processes, to our results of the 16-autumn observation. The model reproduced the differences in the vertical profiles between NO₃⁻ and SO₄²⁻ in the PM_{2.5} well, particularly in the daytime. This revealed that the volatilization of NH₄NO₃ below the canopy under dry conditions enhanced the deposition flux of HNO₃ converted from NH₄NO₃. The DR₃₀₋₁ value of NO₃⁻ calculated by the model was similar to that

observed in the daytime but was smaller than that observed in the nighttime. These results are likely due to the uncertainty in the process of the equilibrium shift of NH₄NO₃ due to the low concentrations of HNO₃ and other nighttime processes.

4. CONCLUSIONS

To better understand the dry deposition process of NO₃⁻ in PM_{2.5} in a forest, we conducted vertical profile measurements of SO₄²⁻ and NO₃⁻ in PM_{2.5}, as well as SO₂, in a forest in suburban Tokyo, Japan, focusing in particular on the daytime/nighttime and leafy/leafless conditions. The observations were performed during the daytime and nighttime during two leafy periods and one leafless period. The vertical gradients of NO₃⁻ were clearly larger than those of SO₄²⁻ in the PM_{2.5} during both the daytime and nighttime, especially for the leafy periods. Moreover, the daytime decreasing rate of NO₃⁻ in the PM_{2.5} below the canopy was larger than that of SO₂ during the leafy periods.

The large NO₃⁻ gradients in the PM_{2.5} were caused by the equilibrium shift from NH₄NO₃ to NH₃ and HNO₃ near the deposition surfaces. In the daytime, the air temperature was higher near the canopy surface during the leafy periods and near the ground surface during the leafless period. These conditions enhanced the volatilization of NH₄NO₃ near the deposition surfaces in the daytime. Moreover, the lower concentration of HNO₃ near the surfaces caused by its fast removal enhanced the volatilization during both the daytime and nighttime. Therefore, NO₃⁻ in the PM_{2.5} was quickly removed by the forest and its vertical gradients were larger than those of SO₄²⁻ in the PM_{2.5}, even to the point of being equal to those of SO₂.

Because the abovementioned chemical processes during dry deposition are not treated in current chemical transport models, future studies focused on the quantification of these processes are required to improve the model accuracy to estimate PM_{2.5} and nitrogen deposition.

ACKNOWLEDGEMENT

We gratefully acknowledge the support of Mr. Takaaki Honjo and Mr. Taiichi Sakamoto (Tokyo University of Agriculture and Technology) in the observations of this

study. We would like to thank Dr. Genki Katata (Ibaraki University), Dr. Atsuyuki Sorimachi (Fukushima Medical University) and Dr. Akira Takahashi (Central Research Institute of Electric Power Industry) for useful discussions. We would also like to thank Enago (www.enago.jp) for the English language review. This work was supported by JSPS KAKENHI Grant Number 16H02933 and the Steel Foundation for Environmental Protection Technology (36th and 37th grants).

REFERENCES

- Ban, S., Matsuda, K., Sato, K., Ohizumi, T. (2016) Long-term assessment of nitrogen deposition at remote EANET sites in Japan. *Atmospheric Environment*, 146, 70–78. <https://doi.org/10.1016/j.atmosenv.2016.04.015>
- Brost, R.A., Delany, A.C., Huebert, B.J. (1988) Numerical modeling of concentrations and fluxes of HNO_3 , NH_3 , and NH_4NO_3 near the surface. *Journal of Geophysical Research*, 93, 7137–7152. <https://doi.org/10.1029/JD093iD06p07137>
- Erismann, J.W., Draaijers, G.P.J. (1995) Atmospheric deposition in relation to acidification and eutrophication. *Studies in Environmental Research*, vol. 63. Elsevier, The Netherlands, pp. 85–97.
- Flechar, C.R., Nemitz, E., Smith, R.I., Fowler, D., Vermeulen, A.T., Bleeker, A., Erismann, J.W., Simpson, D., Zhang, L., Tang, Y.S., Sutton, M.A. (2011) Dry deposition of reactive nitrogen to European ecosystems: a comparison of inferential models across the NitroEurope network. *Atmospheric Chemistry and Physics*, 11, 2703–2728. <https://doi.org/10.5194/acp-11-2703-2011>
- Galloway, J.N., Townsend, A.R., Erismann, J.W., Bekunda, M., Cai, Z., Freney, J.R., Martinelli, L.A., Seitzinger, S.P., Sutton, M.A. (2008) Transformation of the Nitrogen Cycle: Recent Trends, Questions, and Potential Solutions. *Science*, 320, 889–892. <https://doi.org/10.1126/science.1136674>
- Honjo, T., Takahashi, A., Matsuda, K. (2016) Deposition velocity of sulfate and nitrate in $\text{PM}_{2.5}$ above a forest in suburban Tokyo using relaxed eddy accumulation. *Journal of Japan Society for Atmospheric Environment*, 51, 257–265 (in Japanese). <https://doi.org/10.11298/taiki.51.257>
- Huebert, B.J., Luke, W.T., Delany, A.C., Brost, R.A. (1988) Measurements of concentrations and dry surface fluxes of atmospheric nitrates in the presence of ammonia. *Journal of Geophysical Research*, 93, 7127–7136. <https://doi.org/10.1029/JD093iD06p07127>
- Katata, G., Matsuda, K., Sorimachi, A., Kajino, M., Takagi, K. (2020) Effects of aerosol dynamics and gas-particle conversion on dry deposition of inorganic reactive nitrogen in a temperate forest. *Atmospheric Chemistry and Physics*, 20, 4933–4949. <https://doi.org/10.5194/acp-20-4933-2020>
- Kurokawa, J., Ohara, T., Morikawa, T., Hanayama, S., Janssens-Maenhout, G., Fukui, T., Kawashima, K., Akimoto, H. (2013) Emissions of air pollutants and greenhouse gases over Asian regions during 2000–2008: Regional Emission inventory in ASia (REAS) version 2. *Atmospheric Chemistry and Physics*, 13, 11019–11058. <https://doi.org/10.5194/acp-13-11019-2013>
- Matsuda, K., Watanabe, I., Mizukami, K., Ban, S., Takahashi, A. (2015) Dry deposition of $\text{PM}_{2.5}$ sulfate above a hilly forest using relaxed eddy accumulation. *Atmospheric Environment*, 107, 255–261. <https://doi.org/10.1016/j.atmosenv.2015.02.050>
- Morino, Y., Nagashima, T., Sugata, S., Sato, K., Tanabe, K., Noguchi, T., Takami, A., Tanimoto, H., Ohara, T. (2015) Verification of chemical transport models for $\text{PM}_{2.5}$ chemical composition using simultaneous measurement data over Japan. *Aerosol and Air Quality Research*, 15, 2009–2023. <https://doi.org/10.4209/aaqr.2015.02.0120>
- Nakahara, A., Takagi, K., Sorimachi, A., Katata, G., Matsuda, K. (2019) Enhancement of dry deposition of $\text{PM}_{2.5}$ nitrate in a cool-temperate forest. *Atmospheric Environment*, 212, 136–141. <https://doi.org/10.1016/j.atmosenv.2019.05.053>
- Nemitz, E., Sutton, M.A., Wyers, G.P., Otjes, R.P., Mennen, M.G., van Putten, E.M., Gallagher, M.W. (2004) Gas-particle interactions above a Dutch heathland: II. Concentrations and surface exchange fluxes of atmospheric particles. *Atmospheric Chemistry and Physics*, 4, 1007–1024. <https://doi.org/10.5194/acp-4-1007-2004>
- Nemitz, E. (2015) Surface/atmosphere Exchange of Atmospheric Acids and Aerosols, Including the Effect and Model Treatment of Chemical Interactions. Review and Integration of Biosphere-Atmosphere Modelling of Reactive Trace Gases and Volatile Aerosols. Springer, pp. 115–149.
- Ohara, T., Akimoto, H., Kurokawa, J., Horii, N., Yamaji, K., Yan, X., Hayasaka, T. (2007) An Asian emission inventory of anthropogenic emission sources for the period 1980–2020. *Atmospheric Chemistry and Physics*, 7, 4419–4444. <https://doi.org/10.5194/acp-7-4419-2007>
- Sakamoto, T., Nakahara, A., Takahashi, A., Sorimachi, A., Katata, G., Matsuda, K. (2018) Deposition velocity of $\text{PM}_{2.5}$ nitrate and gaseous nitric acid above a forest in suburban Tokyo using relaxed eddy accumulation with denuder sampling technique. *Journal of Japan Society for Atmospheric Environment*, 53, 136–143 (in Japanese). <https://doi.org/10.11298/taiki.53.136>
- Shimadera, H., Hayami, H., Chatani, S., Morino, Y., Mori, Y., Morikawa, T., Yamaji, K., Ohara, T. (2014) Sensitivity analyses of factors influencing CMAQ performance for fine particulate nitrate. *Journal of the Air & Waste Management Association*, 64, 374–387. <https://doi.org/10.1080/10962247.2013.778919>
- Shimadera, H., Hayami, H., Chatani, S., Morikawa, T., Morino, Y., Mori, Y., Yamaji, K., Nakatsuka, S., Ohara, T. (2018) Urban Air Quality Model Inter-Comparison Study (UMICS) for improvement of $\text{PM}_{2.5}$ simulation in greater Tokyo area of Japan. *Asian Journal of Atmospheric Environment*, 12, 139–152. <https://doi.org/10.5572/ajae.2018.12.2.139>
- Sievering, H., Enders, G., Kins, L., Kramm, G., Ruoss, K., Roeder, G., Zelger, M., Anderson, I., Dlugi, R. (1994) Nitric acid, particulate nitrate and ammonium profiles at the Bayerischer

- Wald: evident for large deposition rates of total nitrate. *Atmospheric Environment*, 28, 311–315. [https://doi.org/10.1016/1352-2310\(94\)90106-6](https://doi.org/10.1016/1352-2310(94)90106-6)
- Takahashi, A., Wakamatsu, T. (2004) Estimation of deposition velocity of particles to a forest using the concentration gradient method. *Journal of Japan Society for Atmospheric Environment*, 39, 53–61 (in Japanese). <https://doi.org/10.11298/taiki1995.39.53>
- Van Oss, R., Duyzer, J., Wyers, P. (1998) The influence of gas-to-particle conversion on measurements of ammonia exchange over forest. *Atmospheric Environment*, 32, 465–471. [https://doi.org/10.1016/S1352-2310\(97\)00280-X](https://doi.org/10.1016/S1352-2310(97)00280-X)
- Wyers, G.P., Duyzer, J.H. (1997) Micrometeorological measurement of the dry deposition flux of sulphate and nitrate aerosols to conifer forest. *Atmospheric Environment*, 31, 333–343. [https://doi.org/10.1016/S1352-2310\(96\)00188-4](https://doi.org/10.1016/S1352-2310(96)00188-4)
- Yamazaki, T., Takahashi, A., Matsuda, K. (2015) Differences of dry deposition between sulfate and nitrate in PM_{2.5} to a forest in suburban Tokyo by vertical profile observations. *Journal of Japan Society for Atmospheric Environment*, 50, 167–175 (in Japanese). <https://doi.org/10.11298/taiki.50.167>